Journal of Materials Science & Surface Engineering Vol. 4 (1), 2016, pp 339-341

Contents lists available at http://www.jmsse.org/

Journal of Materials Science & Surface Engineering

Synthesis of Iron Nanopowder and Its Nanocomposites with High Electrical Conductivity and Thermal Stability

R. K. Goyal[1]*, P. Dhoka[2], A. Bora[1], P. Gaikwad[1]

[1]*Department of Metallurgy and Materials Science, College of Engineering, Pune - 411 005, India.*
[2]*Industrial Metal Powders (I) Pvt. Ltd., Shirur, Pune – 412 216, India.*

Article history

Received: 30-Oct-2015
Revised: 19-Jan-2016
Available online: 21-Jan-2016

Keywords:
Nanoparticles,
High energy ball milling,
Nanocomposites,
Conductivity,
Thermal Stability

Abstract

In this work, synthesis of iron nanopowder using planetary ball mill in air atmosphere and its nanocomposites for electromagnetic interference shielding has been discussed. Scanning electron microscope and BET surface area showed a significant decrease in particle size with increasing milling time. The lowest crystallite size determined from X-ray diffractometer was 16 nm. Further, this iron nanopowder was used as reinforcement to prepare polypropylene based nanocomposites using hot pressing. The decomposition temperature, dielectric constant and electrical conductivity of the nanocomposites were increased by more than 100 °C, 65-folds and 1014 times compared to pure polypropylene.

Introduction

Iron (Fe) nanopowder has been used for various applications due to large surface areas to volume ratio [1-3]. There are many methods such as mechanical grinding, spraying, reconstituting oxide powders using CO, pyrolysis of metallic carbonyl compounds, electrochemical deposition, etc., to synthesize iron (Fe) powder. The high energy ball mill has been used to synthesize powders with a few tens of nanometers in size of Fe [1], ZnO [4], SiC [5], and TiC [6]. For example, micro sized SiC powder was reduced to 26 nm after milling of 50 h [5]. TiC nanopowder was synthesized to a crystallite size of around 150 nm by milling both titanium (99.5% purity) and graphite (carbon 99 %) powders together for 16 h [6]. However, internal strain was also found to increase with increasing milling time. It has been reported that the micron sized Fe powder filled polymer composites showed significant improvement in electrical properties [7-11]. It is also true that nano sized fillers have better effect, compared to micron sized fillers, on thermal, electrical and mechanical properties of composites.

In this work, the commercial iron powder with mean size of 40 µm was reduced to nanosized powder using planetary ball mill and the resultant iron nanopowder was added to the polypropylene (PP) matrix by varying its content from 0 to 60 wt% (14.6 vol%) to see its effect on thermal stability and electrical properties. For comparison, 40 wt% micron sized Fe powder filled PP composite was also prepared.

Experimental

Commercial grade electrolytic iron powder with mean size about 40 µm and purity 99.9 % donated by Industrial Metal Powders (I) Pvt. Ltd., Pune, India was milled using a Retsch PM 200 planetary ball mill. Both the ball and vial were made of tungsten carbide. The milling was carried out in air atmosphere at room temperature. The ball to powder weight ratio and the milling speed were 10:1 and 250 rpm, respectively. Small amounts of milled powders were taken out at defined period of times (0 to 28 h) to examine structural and morphological analysis. The Fe powder milled for 28 h was used as reinforcement for fabrication of PP/Fe nanocomposites using solution (xylene as solvent) method followed by hot pressing. Fe powder was suspended first in xylene and sonicated for about 30 min. Then, PP beads were added to the Fe/xylene suspension, stirred for 2-3 h followed by heating. The dried powder was further dried in a vacuum oven at 150 °C for 6 h. The dried nanocomposites powders were hot pressed at 230 ^{0}C.

The particle size (d_{BET}) was estimated on the basis of the Brunauer-Emmett-Teller (Model: Smart Sob) specific surface area (A) using equation: $d_{BET} = 6/(A.\rho)$, where, ρ is the density of Fe. The milled powders were characterized by XRD (Philips X'Pert PANanalytical PW 3040/60) with CuKα radiation. The crystallite size was calculated from the full width at half maxima (FWHM, β_c) of the strongest peak in the pattern using the Scherrer equation (1):

$$d = \frac{0.9\lambda}{\beta_c \cos\theta} \qquad (1)$$

where, λ is the wavelength of X-ray used and θ the Bragg angle. The β_c value was made free from instrumental error using standard procedure. Field emission scanning electron microscopy (FESEM, Zeiss, ΣIGMA) of milled Fe powder was done at 10 kV. Energy dispersive X-ray spectroscopy (EDS) was done for element analysis. The dielectric constant (Ɛ) was measured using precision impedance analyzer (Wayne Kerr, 6417B) at 1 kHz and

Corresponding author. Tel./fax- +91-20-25507275/+91-20-25507299
E-mail address: rkgoyal72@yahoo.co.in

30 ^{0}C. It was evaluated using the equation; $\varepsilon = (C \times t)/\varepsilon_0 \times S$, where, C is the measured capacitance of the sample, t the thickness of the sample, S the surface area of the sample and ε_0 is the permittivity of free space (8.854×10^{-12} F/m). Volume electrical conductivity was measured using electrometer (Keithley, 6517B) and 7½ digital multimeter (Keithley, 2001) when the resistance (R) of the sample was above and below 1 kΩ, respectively. The conductivity (σ) was calculated using equation; $\sigma = t/(R.S)$. Thermo gravimetric analysis (Perkin Elmer, TGA 4000) was done to determine the thermo-oxidative stability during 50 ºC to 650 ºC at a heating rate of 10 ºC/min in air atmosphere. The temperatures of 10 % weight loss were represented as the degradation temperature (T_{10}) and the char yield obtained at 650 ºC was reported.

Results and Discussion

SEM images of Fe powder milled for 0 to 28 h are shown in Fig. 1a-f, respectively. As shown in Fig. 1, as received iron powder (0 h) indicates irregular shaped particles with size varying from few microns to more than 50 microns. As milling time increases, the particle size decreases significantly due to their repeated fracturing and welding. During ball milling, the progressive accumulation of defects and imperfections lead to decrease in particle size. After 15 h milling time, the particle sizes have been reached to less than 1.0 µm. In addition, particles have high amount of aggregates. After 28 h, the milled powder particles seems to be non-spherical (i.e., irregular) in shapes. Further, we can see that Fe particles have been flattened to thin sheets with thickness less than 100 nm and the width around 1.5 µm indicating aspect ratio around 15. EDS showed that the oxygen content increased from 5% for the as received Fe to 8.4 % for the 28 h milled Fe which confirms the oxidation of Fe during milling. However, EDS and XRD did not show presence of tungsten element from the balls and vial used for milling.

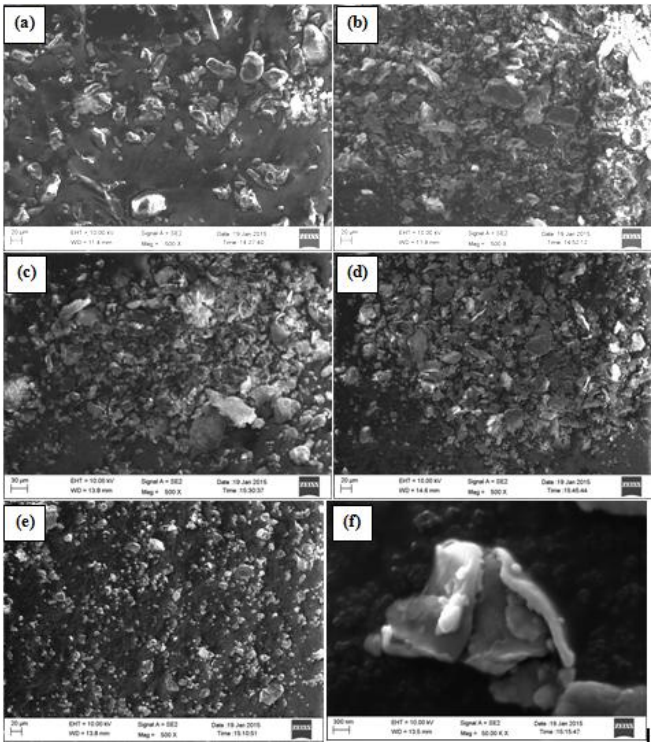

Figure 1: SEM images of iron powder after ball milling time of (a) 0 h, (b) 10 h, (c) 15, (d) 20 h and (e-f) 28 h. Images a-e are taken at 500 × and image f at 50000 ×.

Figure 2 shows that the specific surface area increased from 2.0 m^2/g to 7.8 m^2/g as the milling time increased from 10 h to 28 h and the d_{BET} decreased from > 370 nm to < 98 nm which is in consistent with the results obtained from SEM images. XRD patterns (not shown here) showed sharp diffraction peaks at 2θ = 44.71º and 65.02 º corresponding to diffraction planes of (100) and (200), respectively. In addition, a peak of Fe_3O_4 was also found at 2θ = 48.23º for plane of (331). With increasing milling time, the breadth of the diffracting peaks becomes broader and the peak intensity decreased. The crystallize size of milled powder decreased to 25 nm, 19 nm and 15 nm after milling time of 15 h, 20 h and 28 h, respectively.

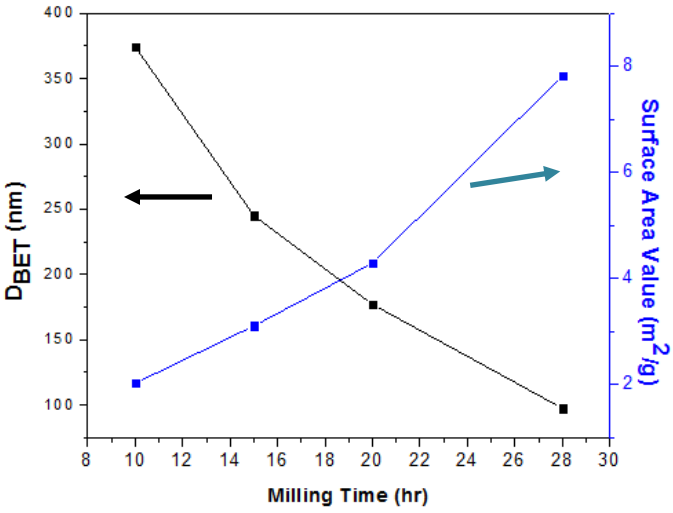

Figure 2: Effect of milling time on average particle size (D_{BET}) and specific surface area

Milled Fe powder with size of less than 100 nm and crystallite size around 15 nm was reinforced into the PP matrix and its electrical and thermal properties were studied. Table 1 shows that the dielectric constant of the nanocomposites increased significantly with increasing Fe content. The increased dielectric constants are due to the higher polarization at the interface which happened due to the presence of well dispersed nano sized Fe particles in the matrix. The dielectric constant of NC-60 increased by more than 65-folds compared to pure PP. The dissipation factor (not shown) of the nanocomposite was also increased with increasing Fe content. The electrical conductivity of the NC-50 and NC-60 nanocomposites was found to be 19.3 S/m and 17.9×10^3 S/m, respectively (Table 1). It indicates that the percolation threshold was obtained at 40 wt% Fe content. It is interesting to see significant increase in conductivity at 7 vol% Fe, despite presence of oxide on Fe particle surface. It is due to the presence of thin Fe sheets (as seen in Fig. 1f) which has higher surface area to volume ratio and helps in forming interconnected 3-dimensional structure in the matrix, hence, facilitates transfer of electrons through the matrix.

Figure 3 shows TGA of the nanocomposites as a function of temperature. As shown in Table 1, the T_{10} for pure PP is 291^{o}C. For 40 wt%, its value increased to 343 $^\circ$C and 391 $^\circ$C for composites containing micron and nano sized Fe, respectively. The maximum decomposition temperature increased from 364 ^{o}C for pure PP to 426 ^{o}C and 437 ^{o}C for NC-40 and NC-60, respectively. Compared to micro-Fe, nano-Fe provides more barriers to the movement of polymer chains and better interaction between Fe and matrix. The char yield of the nanocomposites increased significantly compared to pure PP and it is higher than that of microcomposite (MC-40). It indicates

that nano sized Fe filler provides better thermo oxidative stability.

Table 1: Compositions of the PP/iron nanocomposites and their properties

Sample Code	Vol% Fe in PP matrix	Conductivity (S/m)	Dielectric constant at 1 kHz	Degradation Temperature, T_{10} (°C)	Char yield at 450 °C in air
NC-0 *	0	8.5×10^{-11}	3.0	291	0
NC-40	7.08	11.0×10^{-4}	20	390	48.0
MC-40	7.08	-	-	343	45.0
NC-50	10.26	19.3	30	-	-
NC-60	14.64	17.9×10^{3}	195	391	58.3

* Where NC-X and MC-X represent nanocomposites and composite containing X weight% micro- and nano sized Fe powder, respectively, in the PP matrix.

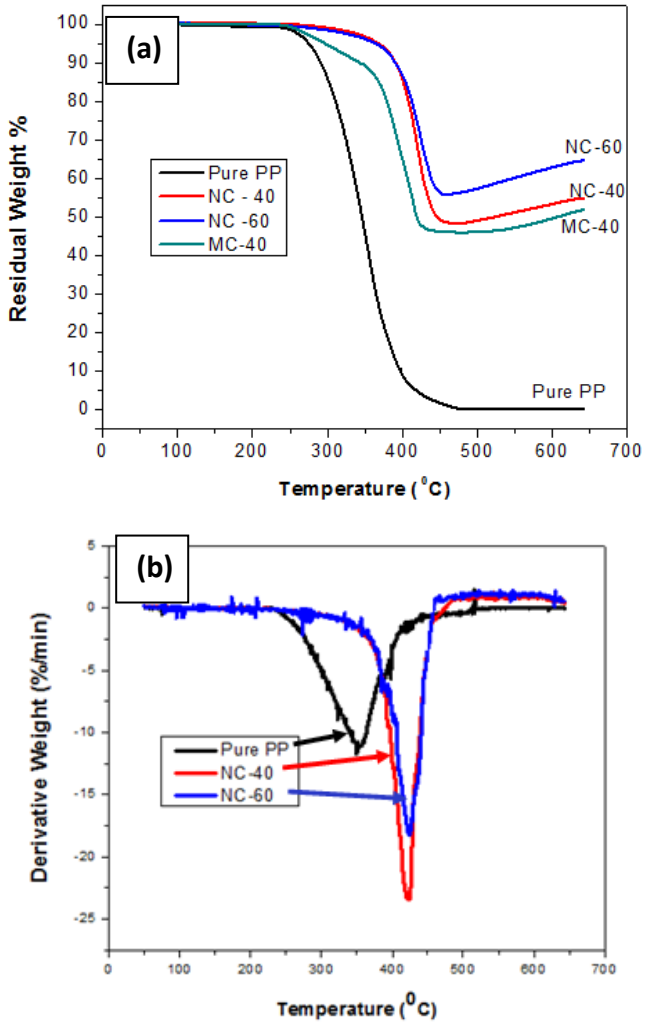

Figure 3: (a) TGA and (b) DTG of PP/Fe nanocomposites as a fun of temperature 341

Conclusions

Based on the results obtained from the experiments following conclusions can be drawn:

1. Nanocrystalline iron powder with size less than 100 nm was successfully synthesized using planetary ball mill. However, XRD and EDS showed presence of iron oxide in nanopowder.
2. PP/Fe nanocomposites containing milled Fe nanopowder were successfully fabricated using solution method followed by hot pressing.
3. The dielectric constant (at 1kHz) and the electrical conductivity of the nanocomposites were increased approximately 65-folds and 10^{14} times, respectively, compared to pure PP.
4. Thermal stability of the nanocomposites increased with increasing Fe content in the PP. For a given wt%, nanocomposite showed better thermal stability compared to microcomposites.

Acknowledgments

M/s Industrial Metal Powders (I) Pvt. Ltd., Pune, India is highly acknowledged for donating electrolytic grade iron powder for this research.

References

1. Bui TT, Le XQ, Nguyen VT. Nanosci Nanotech 2013;4:254-261.
2. JF de Carvalho, SN de Medeiros, MA Morales. Appl Surf Sci 275 (2013) 84–87.
3. Zhang W-X. J Nanoparticle Res 2003;5:323-332.
4. Amirkhanlou S, Ketabchi M, Parvin N. Materials Letters 2012;86:122–124.
5. Rao JB, Catherin GJ, Rao DV, Raju BN. Int J Eng Sci Tech 2011;3:82-88.
6. Rahaei M, Kazemzadeh A, Ebadzadeh T. Powder Tech 2012;217:369–376.
7. Fritcsch SR. J Nanotech 2012;12:1247-1268.
8. Al-Aqrabawi FS, Zihlif AM, Elimat ZM. J Mater Sci: Mater Electron 2013;24:1690–1695 (PS-Fe).
9. Acosta JL, Ojeda MC, Río C del. Polymer Bulletin 2006;57:199–206.
10. Zhang Y, Wang Ya, Deng Y, Li M, Bai J. Materials Letters 2012;72: 9–11.
11. Chameswary J, Jithesh K, George S, Raman S, Mohanan P, Sebastian MT. Mater Lett 2010;64:743-745.